Supplementary Material:

A molecularly imprinted electrochemical sensor based on dual functional monomers for selective determination of nimodipine

Ying Wang [a], Xuyuan Sun [a], Minmin Liu [a], Zhengyuan Dai [a], Xiaoyu Yang a, Li Li [a,*], Yaping Ding[a,*]

a Department of Chemistry, College of Sciences, Shanghai University, Shanghai, 200444, PR China

* Corresponding author.

E-mail addresses: lilidu@shu.edu.cn (L. Li), wdingyp@sina.com (Y. Ding).

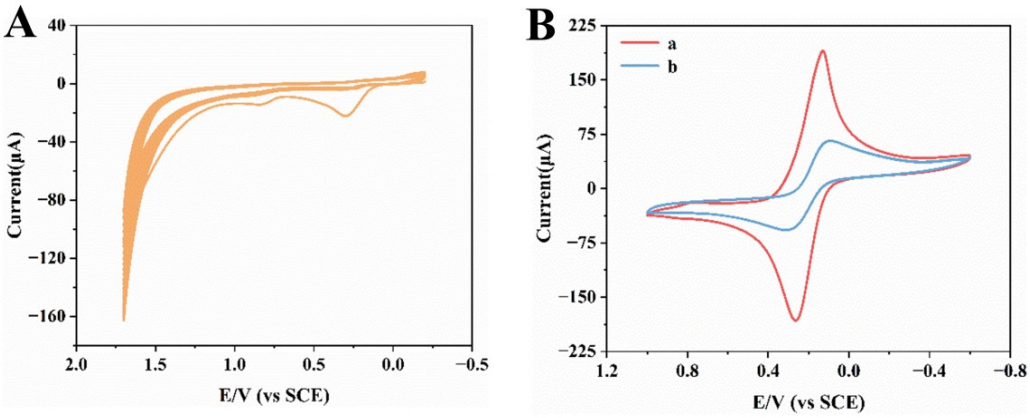

Fig. S1 (A) The cyclic voltammetry curves of MIP membrane electropolymerized on the electrode. (B) CV curves before and after polymerization.

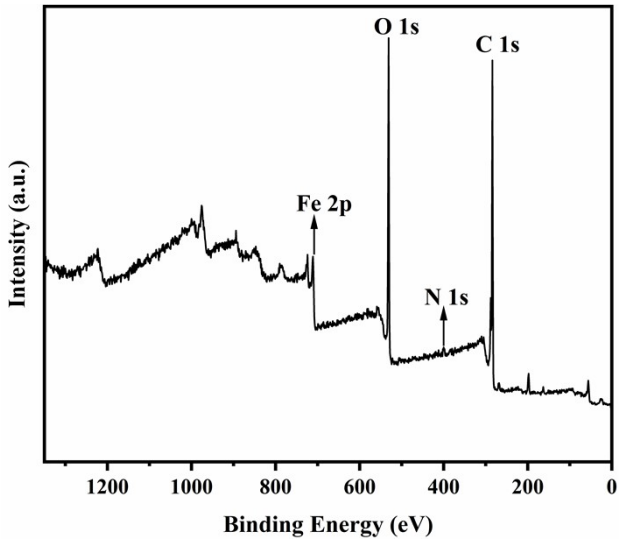

Fig. S2. XPS survey spectrum of Fe-MOF-N-CNT.

Electrochemical impedance spectroscopy (EIS) study of different modified electrodes

As shown in Fig. S3, the EIS curve consists of a semicircle and a line, which represents the charge transfer and diffusion process, respectively. The smaller charge transfer resistance (R_{ct}) value, the better the conductivity. Compared with bare GCE (curve a, R_{ct}=334 Ω), Fe-MOF-N-CNT (curve b, R_{ct}=110 Ω) shows a smaller R_{ct}, indicating that the material has a good electrical conductivity. After the electropolymerization of MIP (curve c, R_{ct}=860 Ω), the R_{ct} value increases significantly due to the non-conductivity of MIP. When the template molecules NMD are eluted (curve d, R_{ct}=160 Ω), the formed imprinted cavities are contributing to the electron transfer, the R_{ct} value decrease. Finally, after adsorption of the template molecules NMD (curve e, R_{ct}=694 Ω), the electron transfer channel is blocked, resulting in the deterioration of the conductivity and the increase of R_{ct} value. Curve f shows the experimental result of NIP/Fe-MOF-N-CNT/GCE.

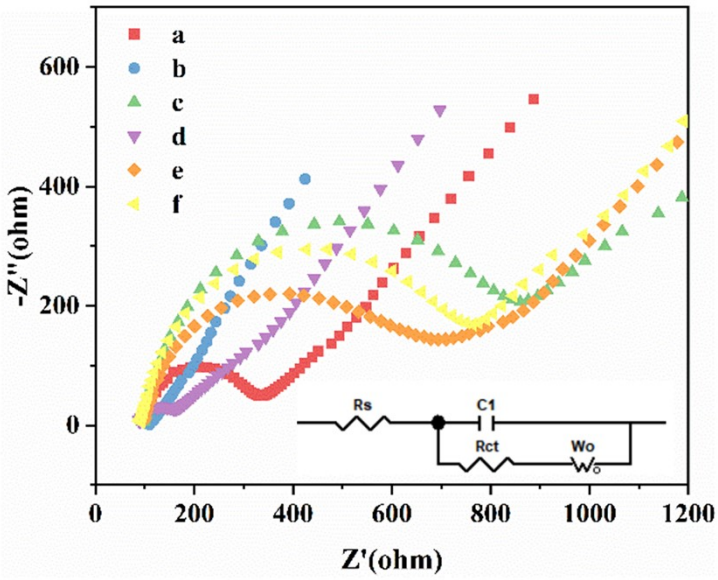

Fig. S3. EIS curves of (a) bare GCE, (b) Fe-MOF-N-CNT/GCE, (c) MIP-dual/ Fe-MOF-N-CNT/GCE before elution, (d) MIP-dual/ Fe-MOF-N-CNT/GCE after elution, (e) MIP-dual/Fe-MOF-N-CNT/GCE after adsorption and (f) NIP/Fe-MOF-N-CNT/GCE in 5 mM $[Fe(CN)_6]^{3-/4-}$ and 0.1 M KCl solution.

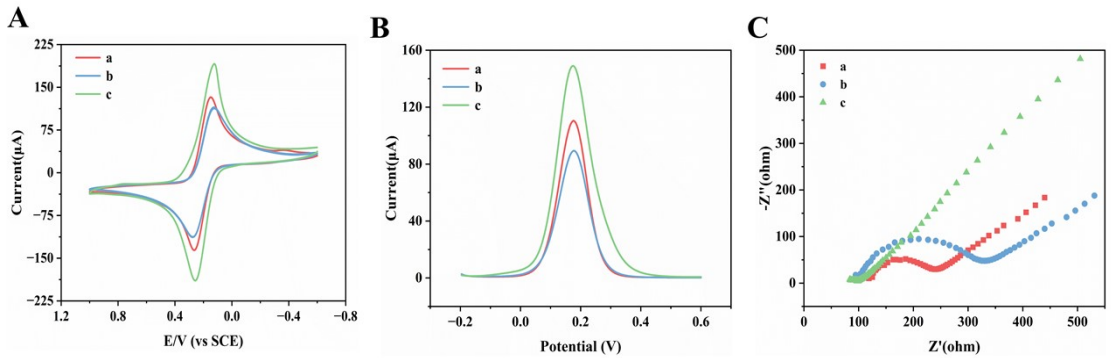

Fig. S4. (A) CV, (B) DPV and (C) EIS curves of (a) bare GCE, (b) Fe-MOF/GCE and (c) Fe-MOF-N-CNT/GCE in 5 mM $[Fe(CN)_6]^{3-/4-}$ and 0.1 M KCl solution.

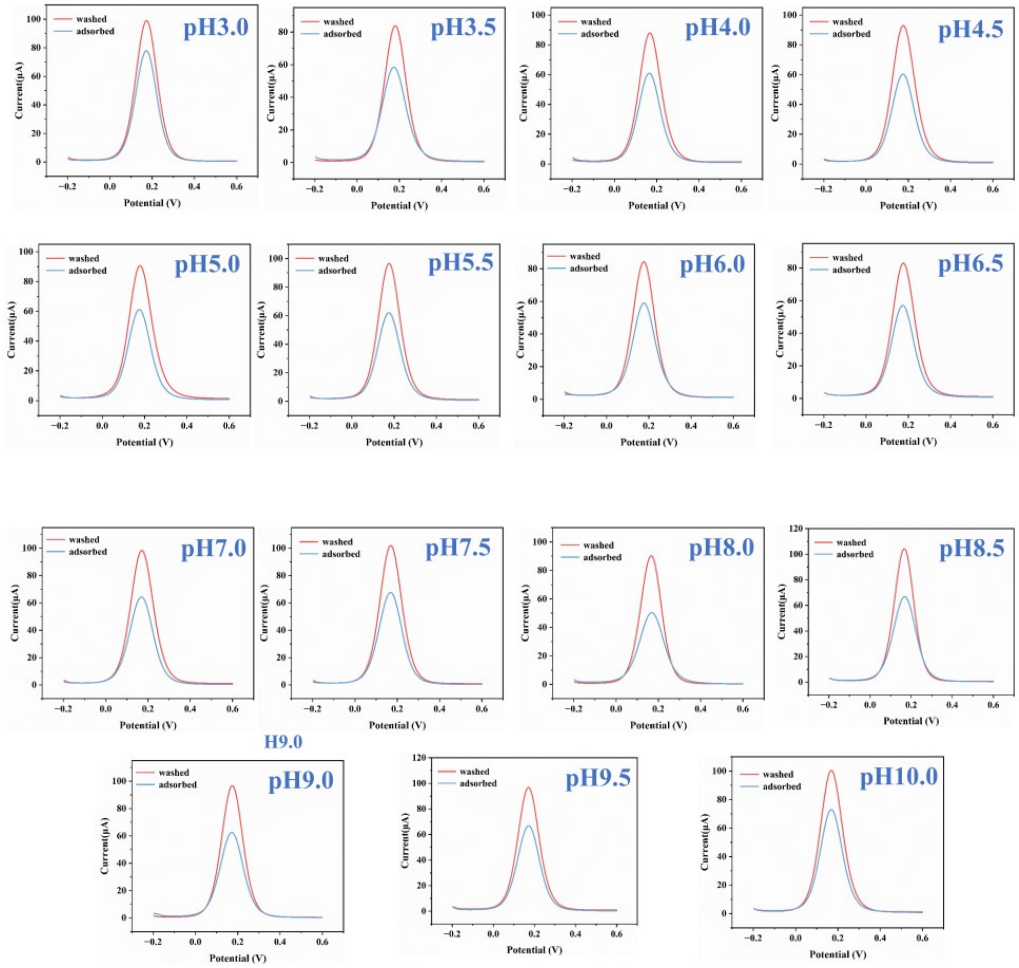

Fig. S5 DPV curves at different pH values from 3.0- 10.0.

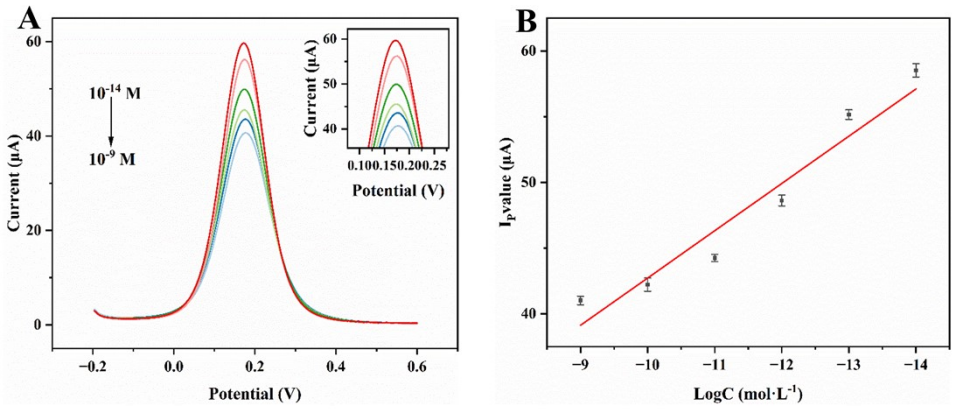

Fig. S6. (A) DPV of NIP/Fe-MOF-N-CNT/GCE with different NMD concentration (from 1.00 × 10^{-14} to 1.00 × 10^{-9} M. (B) Linear relationship between the I_P value of NIP/Fe-MOF-N-CNT/GCE and the logarithm of NMD concentration (from 1.00 × 10^{-14} to 1.00 × 10^{-9} M).

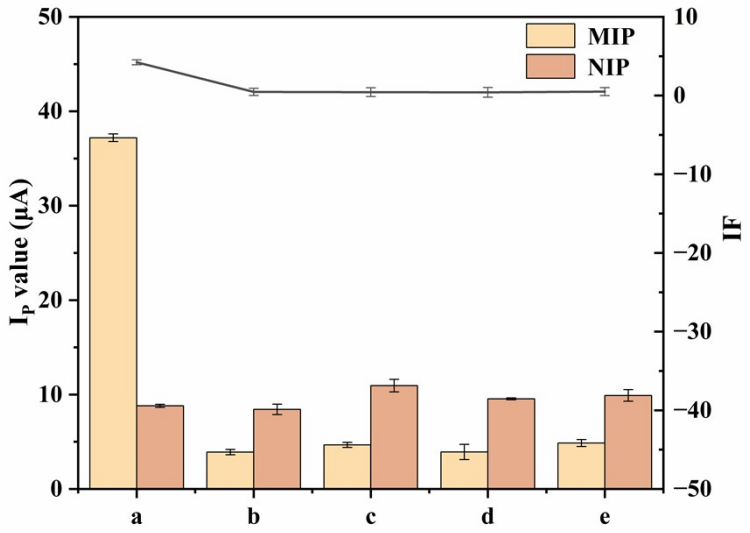

Fig. S7. The imprinting factor of (a) NMD, (b) nifedipine, (c) amlodipine, (d) nisodipine, (e) felodipine corresponding to MIP-dual/Fe-MOF-N-CNT/GCE and NIP/Fe-MOF-N-CNT/GCE.

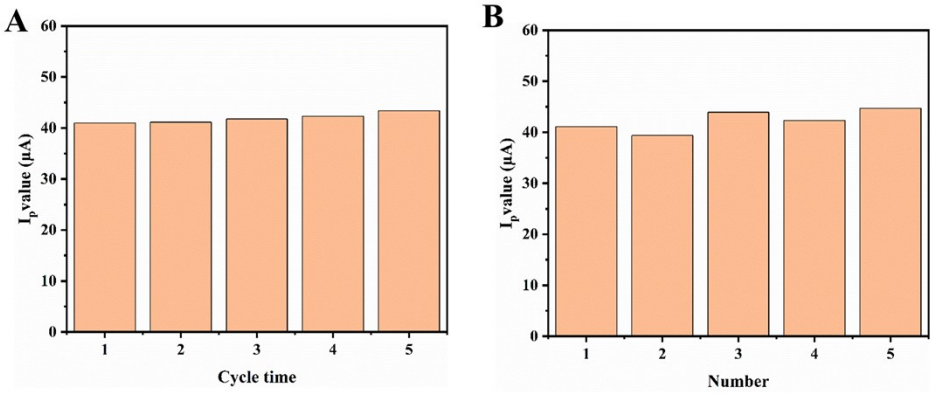

Fig. S8. The (A) repeatability and (B) reproducibility of MIP-dual/Fe-MOF-N-CNT/GCE sensor.

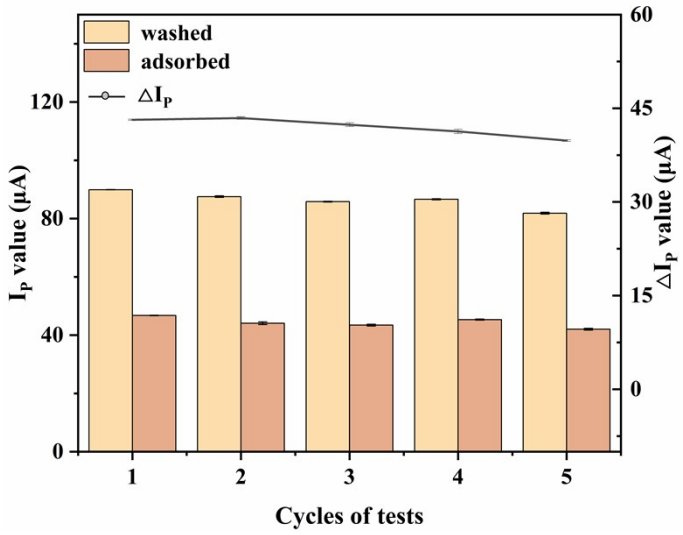

Fig. S9. The reusability of MIP-dual/Fe-MOF-N-CNT/GCE sensor.

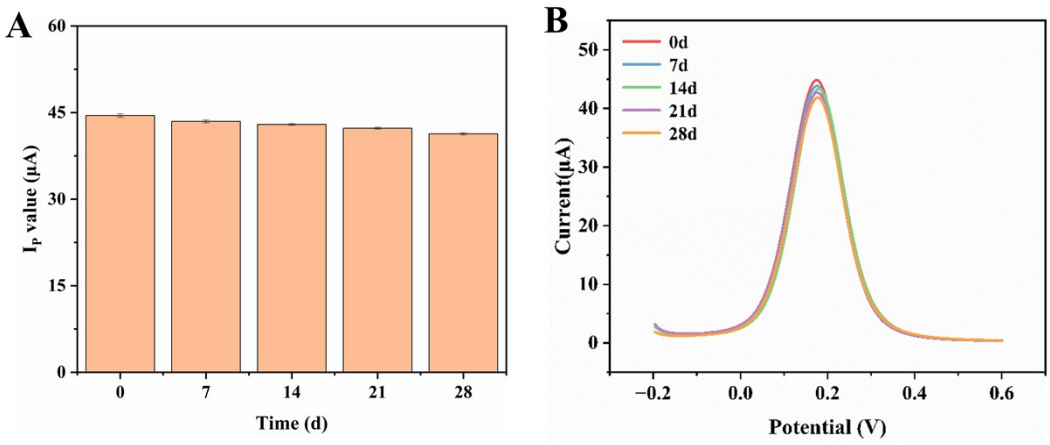

Fig. 10. (A) Stability of MIP-dual/Fe-MOF-N-CNT/GCE sensor. (B) The DPV curves of the sensor's stability.

Table S1

The repeatability and reproducibility experiment of MIP-dual/Fe-MOF-N-CNT/GCE sensor.

	I_{P1} (μA)	I_{P2} (μA)	I_{P3} (μA)	I_{P4} (μA)	I_{P5} (μA)	RSD (%)
The same sensor	40.95	41.15	41.76	42.27	43.61	2.53
Different sensors	41.08	39.37	43.91	42.34	44.66	5.05